Proceedings HTR2006:
3rd International Topical Meeting on High Temperature Reactor Technology
October 1-4, 2006, Johannesburg, South Africa

C00000059

MODEL OF PARTICLE RESUSPENSION IN TURBULENT FLOWS

Marek M. Stempniewicz
NRG Arnhem, Utrechtseweg 310, P.O. Box 9034
6800 ES Arnhem, The Netherlands

Ed M.J. Komen
NRG Petten, Westerduinweg 3, P.O. Box 25
1755 ZG Petten, The Netherlands

ABSTRACT

The graphite dust that will be generated in an HTR/PBMR during normal reactor operation will be deposited inside the primary system and will become radioactive due to sorption of fission products. A significant amount of radioactive dust may be resuspended and released to the environment in case of LOCA. Therefore accurate particle resuspension models are required for HTR/PBMR safety analyses

Thermal-hydraulic safety analyses of HTR/PBMR type reactors are typically performed using computer codes such as FLOWNEX, MELCOR, or SPECTRA. None of these codes has currently a well tested mechanistic resuspension model.

Based on a review of available resuspension models performed at NRG a dynamic resuspension model based on the Vainshtein et al. was selected for implementation into a thermal-hydraulic system code. The resuspension model formulation of Vainshtein et al. has been extended in such way that other formulations, for example the Rock'n Roll model, may easily be defined and used within the general model framework.

The developed resuspension model has been implemented into the SPECTRA thermal-hydraulic system code. Several test calculations were performed, including comparisons of the numerical SPECTRA results with the analytical solutions obtained by means of MathCAD. Furthermore, comparisons with the experimental results of the Reeks and Hall and STORM experiments were made. It was concluded that the model gives quite good results for a number of tests.

The key factor in successful resuspension predictions is a good knowledge of the adhesion force and it's distribution for dust particles deposited on rough surfaces. Theoretical considerations may lead to helpful expressions for the adhesive forces under a variety of conditions. However they cannot be reliably used yet for the assessment of the safety of a Nuclear Power Plant. Therefore, experimental data is needed that will allow to obtain adhesion force distributions for the materials and corresponding surfaces roughness of the components in an actual PBMR plant.

Such experiments will make it possible to calibrate the model, by supplying the adhesion force data, and to verify the developed model. Such experiments will be performed by PBMR.

1 INTRODUCTION

In an HTR/PBMR, graphite dust is generated during normal reactor operation due to pebble-to-pebble scratching. This dust will be deposited throughout the primary system. Furthermore, the dust will become radioactive due to sorption of fission products released, although in very small quantities, during normal operation. In case of a LOCA, a significant amount of radioactive dust may be resuspended and released to the environment. Resuspension of deposited particles is therefore a key issue in HTR/PBMR safety analyses. Consequently, accurate models of particle resuspension need to be present in the thermal-hydraulic system codes that will be used for the HTR/PBMR safety analyses in the future. Thermal-hydraulic analyses of HTR/PBMR type reactors are typically performed using computer codes such as FLOWNEX, MELCOR, or SPECTRA. None of these codes has currently a well tested mechanistic resuspension model.

NRG has performed a review of available resuspension models. The dynamic resuspension models of Vainshtein et al., Reeks Reed and Hall (RRH), and the Rock'n Roll resuspension model were reviewed in more detail. A dynamic resuspension model based on Vainshtein et al. was selected for implementation into a thermal-hydraulic system code. The resuspension model formulation of Vainshtein et al. has been extended in such way that other formulations (for example the Rock'n Roll model) may easily be defined and used within the general model framework.

The developed resuspension model is a well documented and easy to use set of subroutines that may be relatively easily implemented into any thermal-hydraulic or severe accident code. The model has been implemented into the SPECTRA thermal-hydraulic system code [1]. SPECTRA is a general purpose thermal-hydraulic code, developed at NRG.

The resuspension model is shortly described in section 2. A detailed description is provided in reference [1]. Verification of the model was performed firstly by comparing the numerical results with analytical solutions obtained by means of the MathCAD program. Validation of the model was performed by performing simulations of the resuspension experiments of Reeks and Hall and the STORM Test SR11 (ISP-40). The verification and validation results are described in section 3. Finally, sections 4 and 5 provide the summary and conclusions respectively.

2 RESUSPENSION MODEL

The mechanistic resuspension model is based on the work of Vainshtein et al. [2], Reeks et al. [3] and a review of models presented in [4]. In analogy with kinetics models for the desorption of molecules from a surface, the model is based on the assumption that a particle is detached from a surface when it has accumulated enough potential energy to escape from the potential energy well. Such considerations lead to the following formula for the resuspension rate:

$$R_m = f_0 \exp\left[-\frac{Q}{2\langle PE\rangle}\right]$$

f_0 is the typical frequency of vibration [1/s], Q is the height of the surface adhesion potential well, and $\langle PE\rangle$ is the average potential energy of a particle in the well.

In the model of Vainshtein et al. a formula for the resuspension rate is obtained for surfaces where there is a spread of the adhesive forces due to surface roughness. In the present numerical model the continuous spread of the adhesion force is divided into a discrete number of sections, with constant adhesion force in each section. The model keeps track of the particles separately for each section of the adhesion force. During resuspension the adhesion force distribution changes, as the particles with low adhesion forces are resuspended easier (and therefore faster) than the particles with high adhesion forces.

Reference [2] shows that the potential energy, $\langle PE\rangle$, may be expressed in terms of the drag force, F_d, and the height of the potential well, Q, may be found as a function of the tangential pull-off force, $F_{a\tau}$, which in turn is determined by the adhesion force, F_a, as will be shown below.

$$R_m = f_0 \exp\left[-\left(\frac{F_{a\tau}}{F_d}\right)^{x_F}\right]$$

The power x_F has a default value of 4/3. The individual terms in the above formula are described subsequently in the sections below; the frequency of vibration, f_0, in section 2.1, the tangential pull-off force, $F_{a\tau}$, in section 2.2, the adhesion force, F_a (needed for $F_{a\tau}$ calculation) in section 2,3, 2.4, and 2.5, the drag force, F_d, in section 2.6. The model may optionally use a lift force in combination with the drag force. The lift force and the use of a combination of forces is described in section 2.7 and 2.8. Finally section 2.9 gives description of the extended resuspension model, which offers a more general formula through which a model like the Rock'n Roll may be built.

2.1 Frequency of Vibration, f_0

The frequency of vibration, f_0, is given by [2]:

$$f_0 = \frac{\rho_g u_\tau^2}{300\mu_g}$$

u_τ is the friction velocity, [m/s], equal to:

$$u_\tau = \sqrt{f/8}\cdot V_g$$

In the model the formula for f_0 is written as:

$$f_0 = C_{f0}\frac{f}{8}\frac{\rho_g V_g^2}{\mu_g}$$

C_{f0} is a user-defined parameter with the default value of $1/300 = 3.33\times10^{-3}$. An option is available to make f_0 a constant value. In order to achieve that, a negative number should be entered for C_{f0}. In such case f_0 will be equal to:

$$f_0 = \left|C_{f0}\right| \qquad if\ C_{f0} < 0.0$$

2.2 Tangential Pull-off Force, $F_{a\tau}$

The tangential pull-off force is equal to [2], [3]:

$$F_{a\tau} = C_{Fa}\cdot\frac{F_a^{3/2}}{D_{eff}^{1/2}\cdot\chi^{1/2}}$$

C_{Fa} is a user-defined parameter with the default value of 2.0. F_a is the adhesion force, described below. The spring stiffness, χ, is given by the Johnson, Kendall, and Roberts (JKR) model, as described in [3]:

$$\chi = C_\chi\cdot K^{2/3}\cdot D_{eff}^{1/3}\cdot F_a^{1/3}$$

C_χ is a user-defined parameter with the default value of 1.13, while K is given by:

$$K = \frac{4}{3}\left(\frac{1-\nu_p^2}{E_p}+\frac{1-\nu_s^2}{E_s}\right)^{-1}$$

ν_i and E_i are Poisson's ratio and Young modulus respectively. The subscripts p and s stand for the particle material and the surface material respectively. These parameters are user-defined. The values may be found in material handbooks.

The D_{eff} represents effective particle diameter, which is proportional to the particle true diameter, D_p, if $D_p \ll r_{as}$, and is proportional to $2r_{as}$ if $r_{as} \ll D_p$. The D_{eff} is calculated for each particle size section and each F_a-section from:

$$D_{eff} = \frac{1}{\frac{1}{x_p D_p}+\frac{1}{x_{as}2r_{as}}}$$

x_p and x_{as} are user-defined multipliers, D_p is the particle diameter, [m], while r_{as} is the asperity radius, [m].

An option is available to use a scaled adhesion force, F_a, with the scaling factor equal to the absolute value of C_{Fa}:

$$F_{a\tau} = \left|C_{Fa}\right|\cdot F_a \qquad if\ C_{Fa} < 0.0$$

2.3 Adhesion Force Distribution

Surface roughness leads to reduction and spread of the adhesive force, F_a. The spread is a consequence of a spread in the surface roughness. The adhesion force is typically assumed to have the lognormal distribution:

$$\varphi_a(F_a) = \frac{1}{\sqrt{2\pi}} \cdot \frac{1}{F_a \ln(\sigma_a)} \cdot \exp\left(-\frac{1}{2} \cdot \left[\frac{\ln(F_a / \langle F_a \rangle}{\ln(\sigma_a)} \right]^2 \right)$$

Physically the value of $\varphi(F_a)$ gives the fraction of deposited particles that are attached to the surface with the adhesion force equal to F_a per unit adhesion force. If F_a is expressed in [N], then $\varphi(F_a)$ is in [1/N]. Usually F_a, is scaled by some reference value. In this case both F_a and $\varphi(F_a)$ are dimensionless. Examples of the lognormal distribution are shown in Figure 1.

In the model the spread of the adhesion force is represented by using a discrete number of intervals, called the "adhesion force sections", or shortly the "F_a-sections". The typical number of F_a-sections that is applied in the model is between 50 and 100.

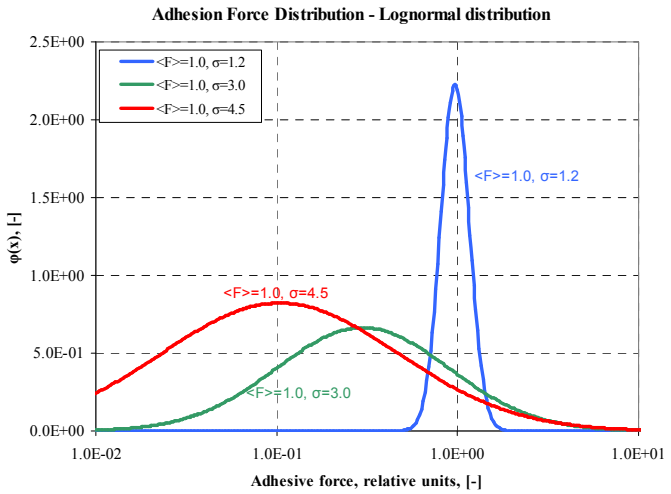

Figure 1 Lognormal distributions.

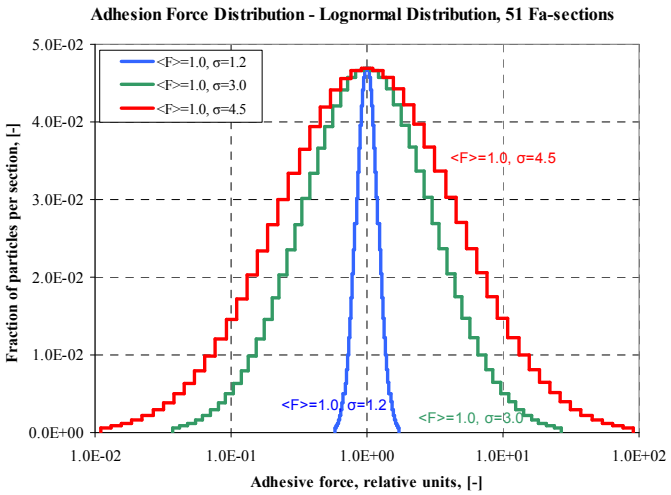

Figure 2 Fraction of particles per F_a-section.

The particle fractions in each F_a-section is obtained by performing a numerical integration of the lognormal distribution over each F_a-section. The resulting particle fractions are shown in Figure 2. Note that the distribution expressed in particle fractions (relative number of particles) per single F_a-section is symmetrical around the mean value, independently of the adhesive spread σ_a (otherwise the mean value would not be the mean value!).

The minimum and maximum values for the "F_a-sections" are determined internally by the model using the following reasoning. It is known that in case of the lognormal distribution practically all (>99%) of the function is located in the interval between:

$$A = \frac{\langle F_a \rangle}{\sigma_a^3}$$

$$B = \langle F_a \rangle \cdot \sigma_a^3$$

The mean value, $<F_a>$, may be either defined by the user or calculated from the correlations built into the model. The adhesive spread factor, σ_a, (standard deviation of the log-normal distribution) is a user-defined parameter. The values of $<F_a>$ and σ_a are used to determine the adhesive force for each F_a-section. Alternatively the adhesive forces may be defined by specifying the asperity size distribution ($<r_{as}>$, σ_{as}). This method is described in the next section. When the adhesion forces are specified directly by $<F_a>$ and σ_a, the asperity size distribution ($<r_{as}>$, σ_{as}) needs to be specified as well, in order to calculate the tangential pull-off forces, F_{at} (it is used to calculate D_{eff} in the formula for χ and F_{at}).

Alternatively the user may specify the adhesive force distribution using a tabular function. With this option any distribution may be defined. This option is useful if the adhesive force distribution is available from measured data.

By default the number of deposited particles is balanced separately for each F_a-section. The user-defined distribution, $\varphi_a(F_a)$, is used only for deposition, to distribute the newly deposited particles in the appropriate F_a-sections. The actual distribution is a result of solving a mass balance for each F_a-section. Of course, if there are no particles left in a given section, then resuspension of this section will stop, $R_m = 0.0$.

2.4 Asperity Radius Distribution

When the adhesion force distribution is determined based on the surface asperity distribution, the asperity distribution is defined instead of the adhesion force itself. This is again done using the lognormal distribution or the tabular distribution. The lognormal distribution is in this case written as:

$$\varphi_{as}(r_{as}) = \frac{1}{\sqrt{2\pi}} \cdot \frac{1}{r_{as} \ln(\sigma_{as})} \cdot \exp\left(-\frac{1}{2} \cdot \left[\frac{\ln(r_{as} / \langle r_{as} \rangle}{\ln(\sigma_{as})} \right]^2 \right)$$

The geometrical mean value, $<r_{as}>$ and the spread factor, σ_{as}, (standard deviation of the log-normal distribution) are user-defined parameters, and may be different for different particle size sections.

If the adhesion force distribution is specified directly - section 2.3 - then only a single value of $<r_{as}>$ is used and applied to all size sections to calculate the tangential pull-off forces, $F_{a\tau}$.

Use of the surface asperities to determine the adhesion forces is applied by Vainshtein et al. [2]. For smooth surfaces, $F_a \sim D_p$. A reduction factor is applied by arguing that for relatively small asperity radii, $r_{as} \ll D_p$, the small asperity may play the role of a particle deposited on a relatively flat surface of the real particle. The resulting reduction factor is equal to $(r_{as}/R_p)=(2r_{as}/D_p)$ and the adhesion force becomes proportional to the asperity radius, $F_a \sim r_{as}$. The original article gives a reduction factor of 0.1.

The assumption that $r_{as} \ll D_p$, may not be applicable for different particle sizes and therefore cannot be applied in general calculation model where the particle size sections may in general vary significantly. In the present model an effective diameter is used, D_{eff}, defined in section 2.2. With this definition

$$F_a \sim \begin{cases} r_{as} & if \quad r_{as} << D_p \\ D_p & if \quad r_{as} >> D_p \end{cases}$$

The approach used in [2] (replacing the particle radius by the asperity radius) is obtained by specifying a large value of x_p and $x_{as} = 1.0$. In such case:

$$D_{eff} = \left. \frac{1}{1/(x_p D_p) + 1/(x_{as} 2r_{as})} \right|_{\substack{x_p \to \infty \\ x_{as}=1.0}} = 2r_{as}$$

and the results become identical to the results of the original model.

2.5 Mean Adhesion Force

The mean adhesion force, $<F_a>$, needs to be calculated if the adhesion force distribution is used (section 2.3) and $<F_a>$ is not specified by the user. In such case $<F_a>$ is determined from a set of built-in correlations, providing the adhesion force from different forces:

The adhesion forces that are taken into account in the model:

- The van der Waals force
- Force arising from the surface tension of adsorbed liquid
- The electrostatic force

Additionally the effect of the gravity force is modelled.

The model applied in CÆSAR [5] predicts that the particle-surface adhesive force is proportional to the particle diameter and inversely proportional to the surface roughness. The adhesion force shown in [5] is reproduced in Figure 3.

In the present model it is assumed that the adhesion may be correlated using the effective particle diameter, D_{eff}, and the surface roughness, R:

$$F_a = \frac{A_1}{R^{x_1}} D_{eff}$$

In the above formula D_{eff} is the effective particle diameter, [m]; R is the surface roughness [m], while A_1 and x_1 are user-defined constants.

An internal limit is applied in SPECTRA for the surface roughness: $R \geq 10^{-9}$. Therefore for the smooth surface: $F_{a,1} = 10^9 \times A_1 \times D_{eff,1}$.

The model applied in CÆSAR predicts that the particle-surface adhesive force is proportional to the particle diameter and inversely proportional to the surface roughness, which means x_1=1.0. Results obtained with the formula applied in SPECTRA with $A_1 = 5\times10^{-10}$ and $x_1 = 1.0$ are shown in Figure 4. The results agree well with the values calculated by CÆSAR (Figure 3). The values shown above are default values of the model, but they can be redefined by the user. Therefore, in the future, if more data on adhesion force is obtained, they will be easy to adopt in the model. A user-defined parameter that has to be supplied is the surface roughness, R, [m].

In the Vainshtein model [2] and the review presented in [4] the following adhesion forces are given for a smooth surface:

$F_a = \pi \cdot \Delta\gamma \cdot D_p$ for small hard particles

$F_a = \frac{3}{4}\pi \cdot \Delta\gamma \cdot D_p$ for large soft particles

$\Delta\gamma$ is the adhesive surface energy, [J/m^2]. For example, if the value of $\Delta\gamma$ is 0.15 J/m^2 (as used in [2]), then:

$F_a = 0.47 \cdot D_p$ for small hard particles

$F_a = 0.35 \cdot D_p$ for large soft particles

To obtain exactly the same values for a smooth surface (R=10^{-9} m) in SPECTRA, the following value of A_1 should be used:

- $A_1 = 0.47\times10^{-9}$ for small hard particles.
- $A_1 = 0.35\times10^{-9}$ for large soft particles.

If $\Delta\gamma$ is 0.56 J/m^2 (as used in [3]), then F_a=1.32×D_p, and:

- $A_1 = 1.32\times10^{-9}$ for large soft particles

The default value, $A_1 = 5.0\times10^{-10}$, is sufficiently close to those values for most practical applications.

The formulae used for the adsorbed liquid, the electrostatic, and the gravity forces are not discussed here. They are described in detail in reference [1]. The total adhesion force is calculated as a sum of the individual adhesion forces. The example shown in Figure 5 shows the total adhesion force for a case where most contributors can be distinguished. Explanation of the behavior observed in Figure 5 is given in [1].

2.6 Drag Force

The drag force, is calculated from the following formula [4]:

$$F_d = X_d \cdot F_d^{'} = X_d \cdot 8.0 \cdot \frac{\mu_g^2}{\rho_g} \cdot \left(D_p^+\right)^2$$

X_d is a user-defined multiplier. D_p^+ is the dimensionless particle diameter, given by:

$$D_p^+ = \sqrt{\frac{f}{8}} \cdot \frac{\rho_g}{\mu_g} \cdot D_p \cdot \left|V_g\right|$$

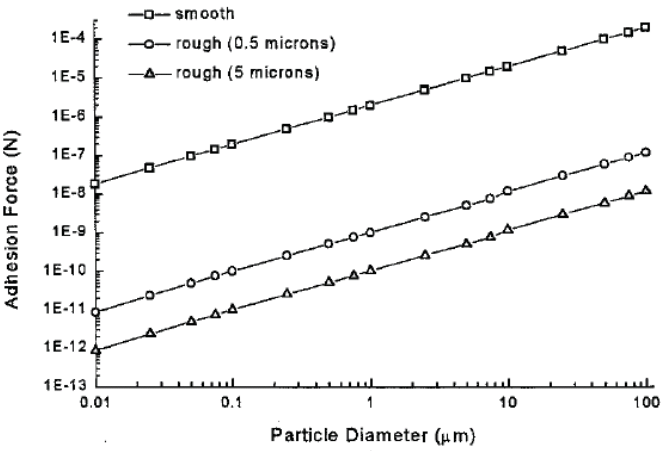

Figure 3 Adhesive force, particles on steel surface [5].

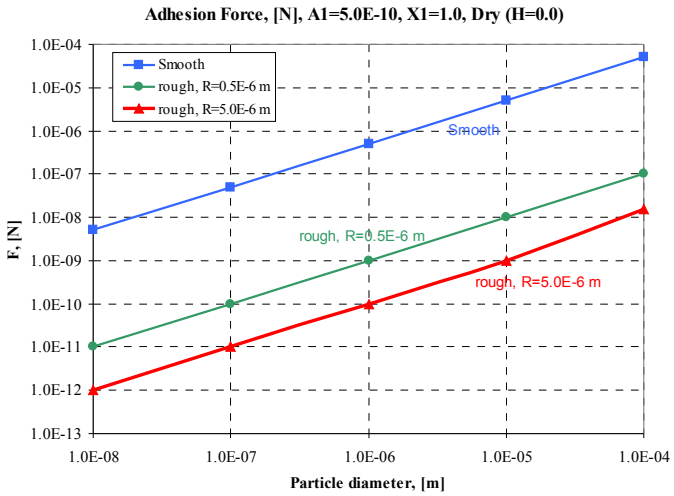

Figure 4 Adhesive force, A_1=5×10^{-10}, x_1=1.0.

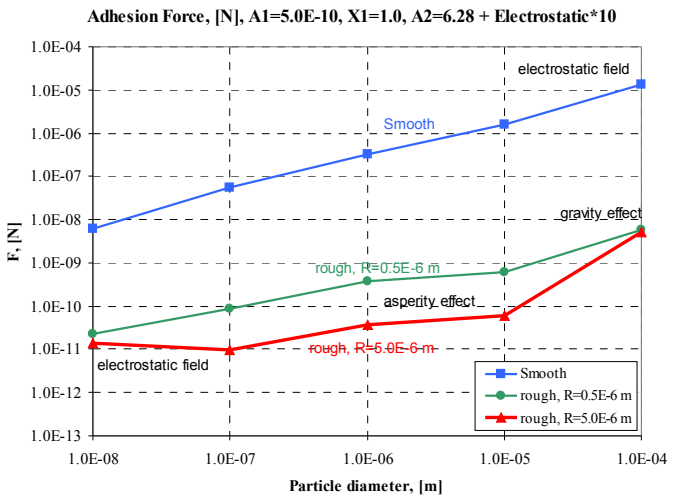

Figure 5 Efect of multiple adhesive forces.

2.7 Lift Force

The lift force, is calculated from the following formulae [4]:

- Expression of Soltani, applied for $D^+ < 8.3$:

$$F_{L,Soltani} = X_L \cdot F'_{L,Soltani} = X_L \cdot 0.975 \cdot \frac{\mu_g^2}{\rho_g} \cdot \left(D_p^+\right)^{3.0}$$

- Expression of Hall, applied for $D^+ > 8.3$:

$$F_{L,Hall} = X_L \cdot F'_{L,Hall} = X_L \cdot 4.215 \cdot \frac{\mu_g^2}{\rho_g} \cdot \left(D_p^+\right)^{2.31}$$

X_L is a user-defined multiplier. The transition point has been chosen at the crossing point of the Soltani's and the Hall's formulae.

2.8 Use of Drag and Lift Forces

The lift force is not used in the Vainshtein resuspension model and is not used by default in the current model. However, an option is available to use the lift force or a combination of the lift and the drag force.

Recall that the resuspension rate is calculated as:

$$R_m(t) = f_0 \exp\left[-\left(\frac{F_{a\tau}}{F_d}\right)^{x_F}\right]$$

This is the default option, where F_d is the drag force calculated using the multiplier X_d (section 2.6). A sum of the drag and the lift force may be used. In such case:

$$R_m(t) = f_0 \exp\left[-\left(\frac{F_{a\tau}}{\left(X_d F'_d\right)+\left(X_L F'_L\right)}\right)^{x_F}\right]$$

Since both X_d and X_L are user defined parameters, any linear combination of drag and lift forces may be achieved in the program.

2.9 Extended Resuspension Model

The extended resuspension model offers a more general formula for the resuspension rate calculation. Instead of the formula described above, the following formula is used:

$$R_m = f_0 \exp\left[-C_1\left(\frac{F_{a\tau} - C_2 F_d}{F_d}\right)^{x_F}\right]$$

C_1 and C_2 are user-defined parameters (default values of 1.0 and 0.0 respectively). A limit is imposed on the difference, such that it never becomes negative ($F_{a\tau} - C_2\, F_d \geq 0.0$).

The extended model may be used for defining an alternative model, for example the Rock'n Roll resuspension model. In the "Rock'n Roll" model (see for example [4]):

$$R_m = f_0 \exp\left[-\frac{1}{2}\left(\frac{F_a - F_{aero}}{0.2 \cdot F_{aero}}\right)^2\right]$$

The aerodynamic force, F_{aero}, is given by:

$$F_{aero} = \left(\frac{r}{a}F_d^{'}\right) + \left(\frac{1}{2}F_L^{'}\right)$$

where $(r/a) \sim 10^2$ [4]. The frequency of vibration:

$$f_0 = 6.58\times10^{-3}\frac{f}{8}\frac{\rho_g V_g^2}{\mu_g}$$

In the Rock'n Roll model the R_m is divided by a term with error function ([4], equation 2.165):

$$\frac{1}{2}\left[1 + errf\left(\frac{F_a - F_{aero}}{\sqrt{2\cdot(0.2\cdot F_{aero})^2}}\right)\right]$$

This term has been neglected here. It is shown in sections 4 and 5 that very small error is made by neglecting this term.

Therefore the following values need to be applied in order to obtain the "Rock'n Roll" model:

$C_1 = 12.5 = (1/2) / (0.2)^2$ $\quad X_d = 10^2 = (r/a)$
$C_2 = 1.0$ $\quad X_L = 0.5$
$C_{Fa} = -1.0$ $\quad x_F = 2.0$
$C_{f0} = 6.58\times10^{-3}$

3 VERIFICATION AND VALIDATION

The resuspension model described in the previous section has been implemented into the thermal-hydraulic system code SPECTRA [1]. Verification and validation of the new code version is described in detail in [1]. Here a short description of the main verification and validation runs is given in section 3.1 through 3.3.

3.1 Comparison with Analytical Solutions

As a first set of tests the model results are compared to "analytical solutions", obtained with help of the MathCAD program and documented in [6]. The analytical solutions presented in [6] were obtained using the Vainshtein model for "large soft particles" with the reduction factor of 0.1. Resuspension of three different particle sizes was calculated:

- Size section 1: $D_p = 0.4\times10^{-6}$ m
- Size section 2: $D_p = 1.5\times10^{-6}$ m
- Size section 3: $D_p = 4.0\times10^{-6}$ m

Three different friction (and gas) velocities were used:

- $u_\tau = 5.0$ m/s $\quad V_g = 153$ m/s
- $u_\tau = 10.0$ m/s $\quad V_g = 309$ m/s
- $u_\tau = 15.0$ m/s $\quad V_g = 459$ m/s

The following assumptions were made for the SPECTRA calculations:

- $A_1 = 3.5\times10^{-10}$ (large soft particles and $\Delta\gamma$=0.15 J/m^2).
- The option of calculating the adhesion force through the asperity distribution (section 2.4) was used.
- The effective diameter was set to be equal to twice the asperity radius, $D_{eff} = 2\ r_{as}$, by specifying a large value of x_p (10^{10})and $x_{as} = 1.0$.
- The lognormal asperity size distribution was selected, with the mean asperity radius is set to 0.1 of the particle radius: $<r_{as}> = 0.1\times(D_p/2)$:
  - Size 1 ($D_p = 0.4\times10^{-6}$ m): $<r_{as}> = 0.20\times10^{-7}$ m
  - Size 2 ($D_p = 1.5\times10^{-6}$ m): $<r_{as}> = 0.75\times10^{-7}$ m
  - Size 3 ($D_p = 4.0\times10^{-6}$ m): $<r_{as}> = 2.00\times10^{-7}$ m
- The same adhesive spread factor (σ_a, = 4.0) was used.
- MathCAD calculations are made using an ideal (instantaneous) velocity step. In SPECTRA however a velocity step always involves a short transient (the same would be the case with any other code, such as MELCOR, RELAP, etc.). In order to be able to compare results even for very short times (of order of 10^{-4} s) a special procedure was applied. A preliminary calculation was performed for each case. Thermal-hydraulic results were stored as the Initial Condition Files (ICF). The real calculations were performed starting from the conditions in the appropriate ICF files (the ICF option in SPECTRA is similar to restarting in RELAP).

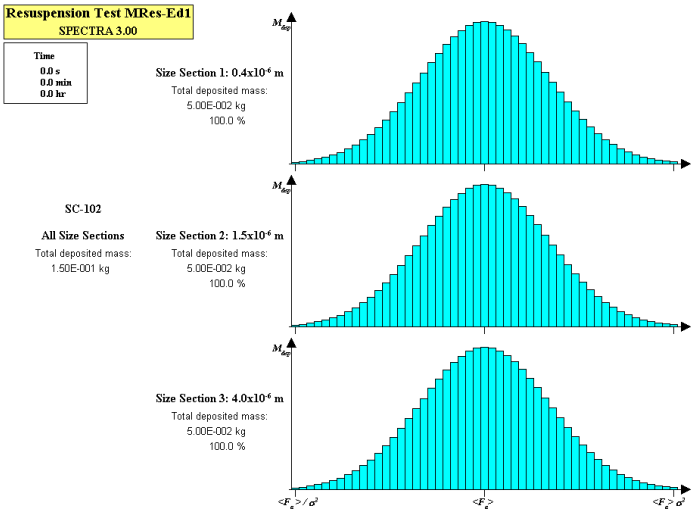

Figure 6 Test Mres-Ed1 F_a-distributions, start time.

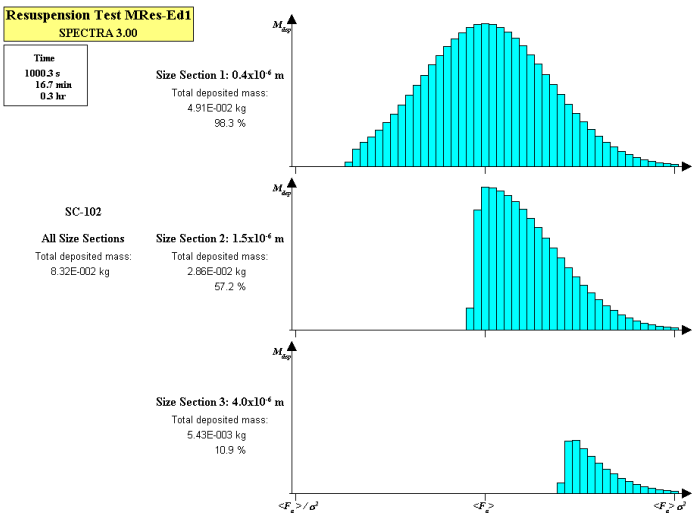

Figure 7 Test Mres-Ed1 F_a-distributions, end time.

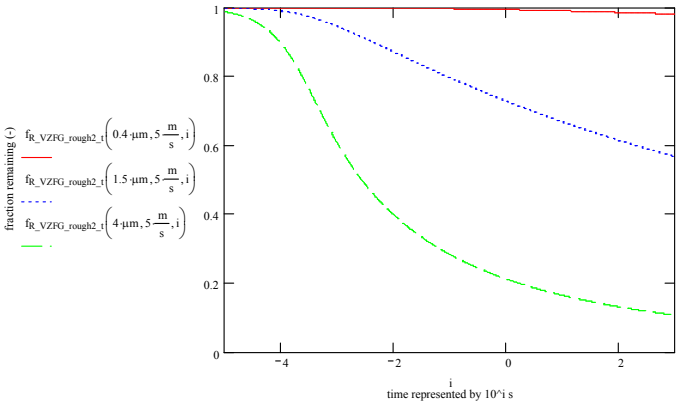

Figure 8 Test Mres-Ed1 MathCAD [6].

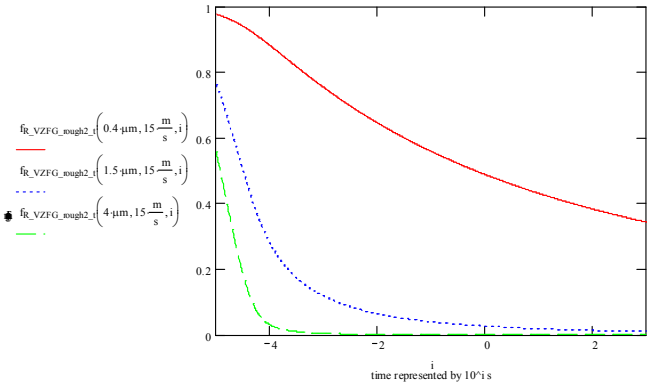

Figure 10 Test Mres-Ed3 MathCAD [6].

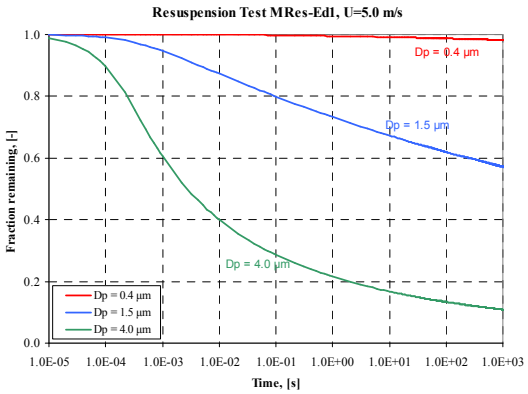

Figure 9 Test Mres-Ed1 SPECTRA.

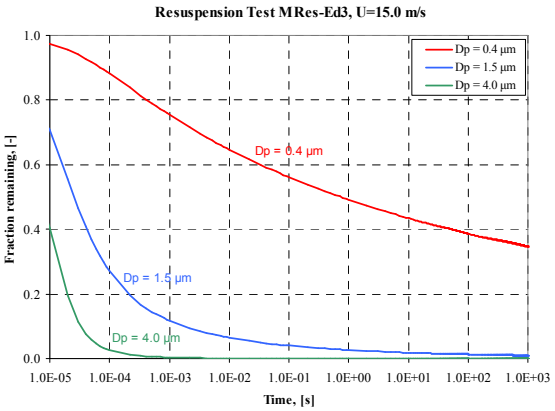

Figure 11 Test Mres-Ed3 SPECTRA.

Results obtained for the first velocity test are shown in Figure 6, through Figure 9. Figure 6 and Figure 7 show F_a-distributions at the start and at the end of the calculations. A lognormal distribution is assumed at the start (Figure 6). At the end the weakly bound particles have been removed, as can be seen in (Figure 7). The large particles (size section 3) are most easily removed, therefore the smallest amount of these particles is present at the end.

Comparisons with MathCAD are shown in Figure 8 and Figure 9. The figures show that an excellent agreement with the "analytical", i.e. the MathCAD solution.

The second velocity test (friction velocity of 10 m/s) is not shown here. Results are discussed in reference [1]. The same agreement was found. Results of the third test is shown in Figure 10 and Figure 11. The agreement between the MathCAD results and SPECTRA results is very good, even for very short times.

For the present tests, the calculation procedure was very careful in order to reproduce the MathCAD results with its instantaneous velocity step (use of ICF). The results shown here prove that the equations were correctly coded in SPECTRA. Therefore, the model is verified.

The next sections present validation of the model against experimental data. Additional verification of some cases against MathCAD is included.

For those cases a "normal" velocity increase steps are made (typically 1 second). This is appropriate for validation against experiments, but the results are not exactly the same as the MathCAD results.

3.2 Reeks and Hall Experiments

The article of Reeks and Hall [7] reports measurements of the short-term resuspension of nominal 10 and 20 µm alumina spheres and graphite particles from a polished stainless-steel flat plate in a fully developed turbulent channel flow for different flow conditions. Below SPECTRA results are compared to the experimental data for the 10 and the 20 µm particles.

3.2.1 "10-µm" particles

The nominal "10-µm" particles had the mean diameter of 12.2 µm. Two resuspension models were used:

- Vainshtein model.
- Rock'n Roll model (built using the "extended mechanistic model" - see section 2.9).

Two options were used:

- Adhesion force distribution (section 2.3) with mean adhesion force, $\langle F_a \rangle$, calculated using the built-in correlations (section 2.5), assuming surface roughness $R = 1.0 \times 10^{-6}$ m.

The mean asperity radius (needed in this case only for conversion of the adhesion force, F_a, to the tangential pull-off force, F_{at}) is equal to:

$$\langle r_{as} \rangle = 1.0 \times 10^{-7} \text{ m}$$

This is a default value [1], based on the reduction factor of 0.1 [2] and particle size of ~1µm.

- Adhesion forces calculated from the asperity distribution (section 2.4). The reduction factors were obtained from the original article [7]: 1/37=0.027 for the "10-µm" particles ([4], Table 4). Therefore the mean asperity radius was defined as:

$$\langle r_{as} \rangle = 0.027 \times \frac{1}{2} \times 12.2 \times 10^{-6} = 1.6 \times 10^{-7} \text{ m}$$

The value of 12.2×10^{-6} is the mean diameter $\langle D_p \rangle$ of the "10-µm" particles.

Considering the adhesive spread factors, σ_a, the original article [7] mentions two different values, namely 2.55 and 10.4.

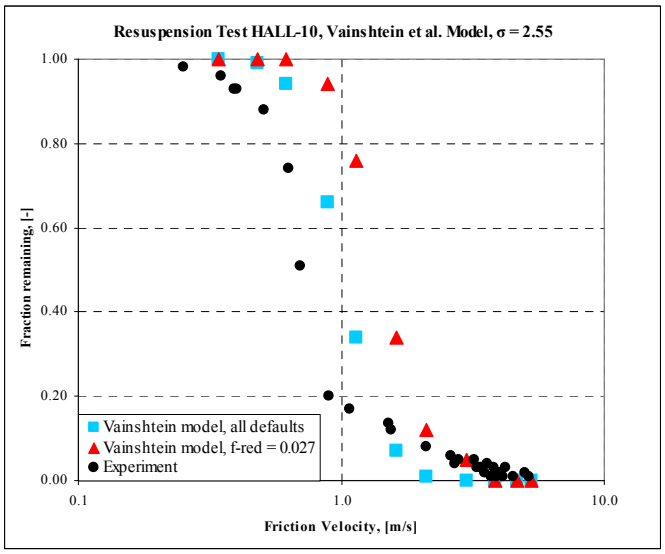

Figure 12 Reeks & Hall, 10 µm, Vainshtein, $\sigma = 2.55$.

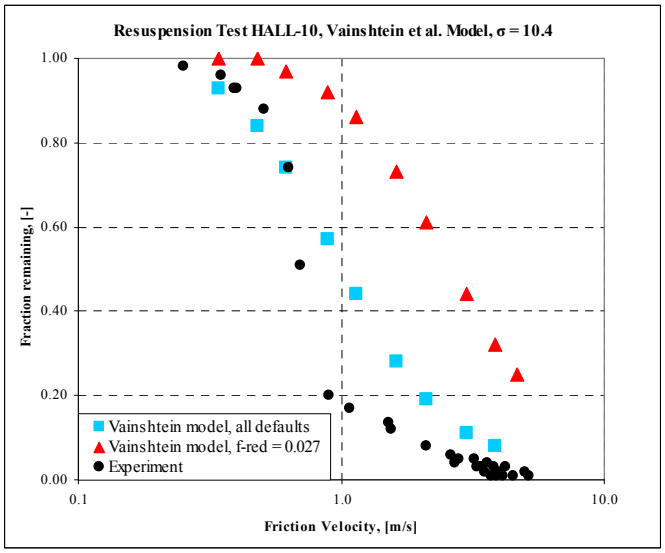

Figure 13 Reeks & Hall, 10 µm, Vainshtein, $\sigma = 10.4$.

The first value is mentioned in relation to the RRH model (Reeks, Reed, and Hall model - which was the basis for the Vainshtein model), while the second is mentioned in relation with the Rock'n Roll model. The spread factors of course determine the adhesion forces, and it is felt that comparing different resuspension models that are using different adhesion forces doesn't make much sense. Therefore both Vainshtein and Rock'n Roll models were run with both adhesive spreads:

- $\sigma_a = 2.55$
- $\sigma_a = 10.4$

Results are shown in Figure 12 through Figure 15. The figures show remaining fractions versus friction velocities. Every point corresponds to a separate run. The remaining fractions were measured 1000 s after a velocity step was made, to ensure that stable (independent of time) values are plotted in the figures (it was found out that this long times are needed for the Vainshtein model; in the Rock'n Roll model remaining fractions become stable much faster [1]).

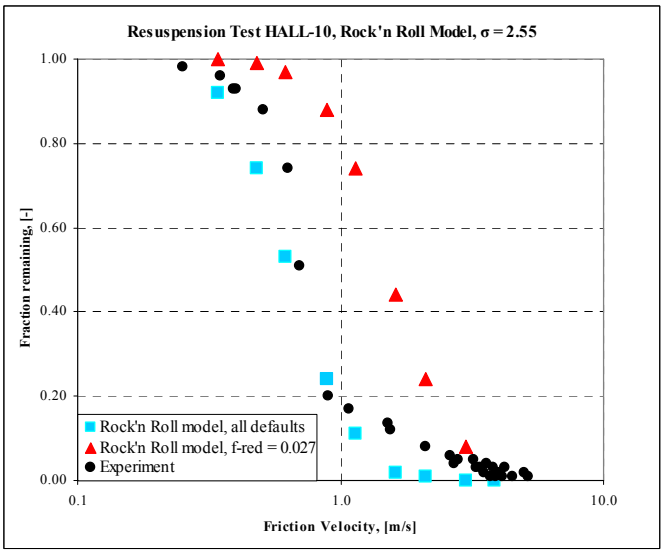

Figure 14 Reeks & Hall, 10 µm, Rock'n Roll, $\sigma = 2.55$.

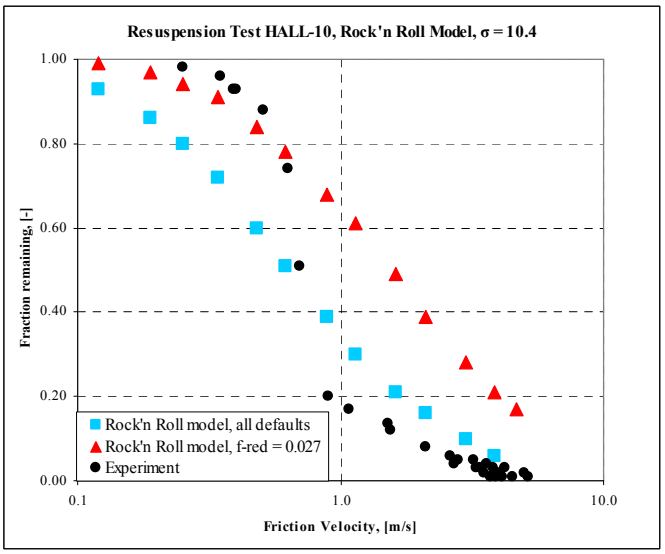

Figure 15 Reeks & Hall, 10 µm, Rock'n Roll, $\sigma = 10.4$.

The following observations can be made:

- Results close to experimental measurement are obtained with the Vainshtein mode with default adhesion force $<F_a>$ calculation. Results obtained with the F_a calculation through asperity size calculation with the reduction factor of f_{red} = 0.027 give too large fraction of remaining particles.
- Results obtained with the adhesive spread of $\sigma_a = 2.55$ give closer match to experimental data than the results of $\sigma_a = 10.4$.
- The Rock'n Roll model with the mean adhesion force $<F_a>$ calculated from the default correlations and σ_a = 2.55 predicted the remaining fractions that are somewhat lower than in experiments. The Vainshtein model with the same assumptions predicted somewhat higher fractions. With these assumptions results of both models are quite close to the measured data.

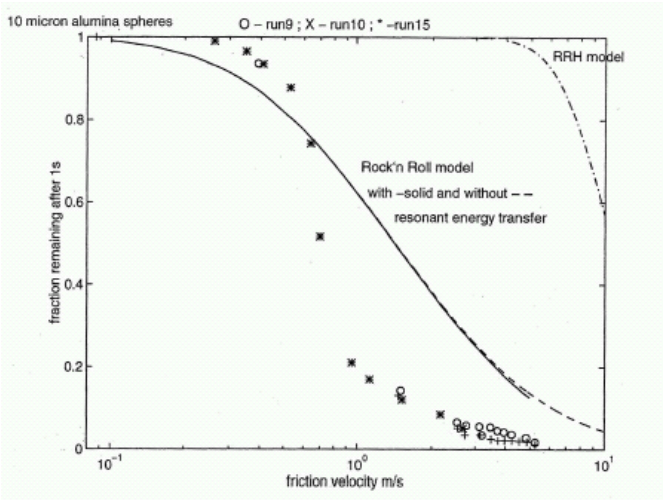

Figure 16 Reeks & Hall, 10-µm, [7].

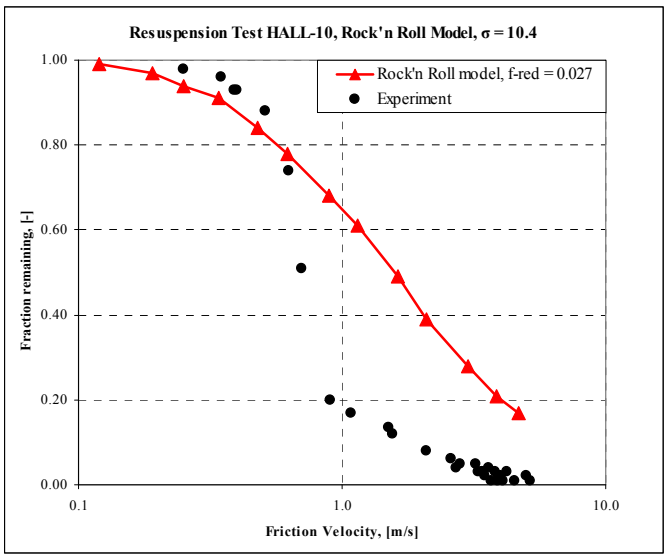

Figure 17 Reeks & Hall, 10-µm, Rock'n Roll, $\sigma = 10.4$.

The results of the Rock'n Roll model, as calculated by SPECTRA are compared to the Rock'n Roll model, as presented in the original article of Reeks and Hall in Figure 16 and Figure 17. The case with σ_a = 10.4 and the Vainshtein approach ($<r_{as}>=f_{red}\times D_p$) with the reduction factor of f_{red} = 0.027 is presented in the article (Figure 16) This case is shown in Figure 17 for comparison (the same case is shown in Figure 15). SPECTRA results for this case agree well with the Rock'n Roll model data presented in [7]. The slope of calculated results is too small compared to the experiment. This is a consequence of applying a large value of σ_a.

In the Rock'n Roll model the R_m is divided by a term with error function (see reference [4]):

$$\frac{1}{2}\left[1+errf\left(\frac{F_a-F_{aero}}{\sqrt{2\cdot(0.2\cdot F_{aero})^2}}\right)\right]$$

This term has been neglected. This term gives the values between 1/2 ($errf(0)=0$) and 1.0 ($errf(\infty)=1$), which can be accommodated by dividing f_0 by 1/2. This is achieved by dividing the input parameter C_{f0} by 1/2. The value of C_{f0} appropriate for the Rock'n Roll model is 6.58×10^{-3} (see section 2.9). Division by 1/2 gives $C_{f0} = 13.2\times10^{-3}$ Sensitivity calculations were performed with this parameter. Results of such sensitivity calculations are shown in Figure 18. It is clearly seen that the effect of this term is very small, in any case negligible compared to the discrepancy between the model prediction and the measured data. This small effect may at first seem surprising, since a factor of up to 2.0 is neglected in the resuspension formula. Explanation of this surprisingly small effect is given below.

In the Rock'n Roll model, the resuspension is quite rapid, more rapid than in the Vainshtein model. This is seen in Figure 19, where the remaining fractions of the deposited particles are plotted versus time.

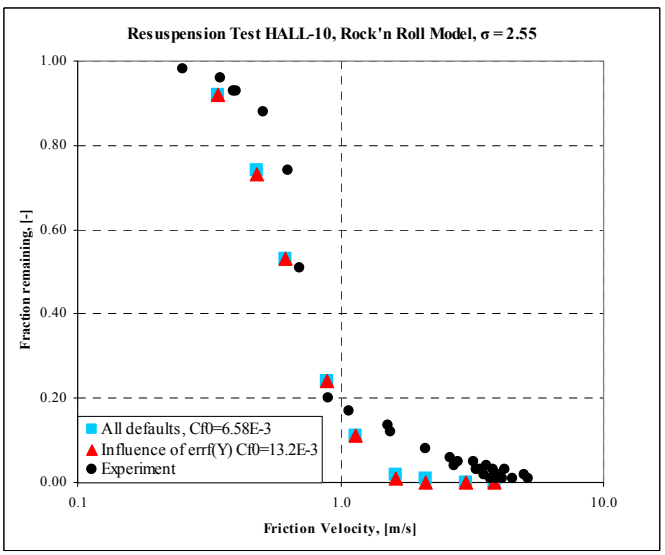

Figure 18 Influence of neglecting errf, Rock'n Roll.

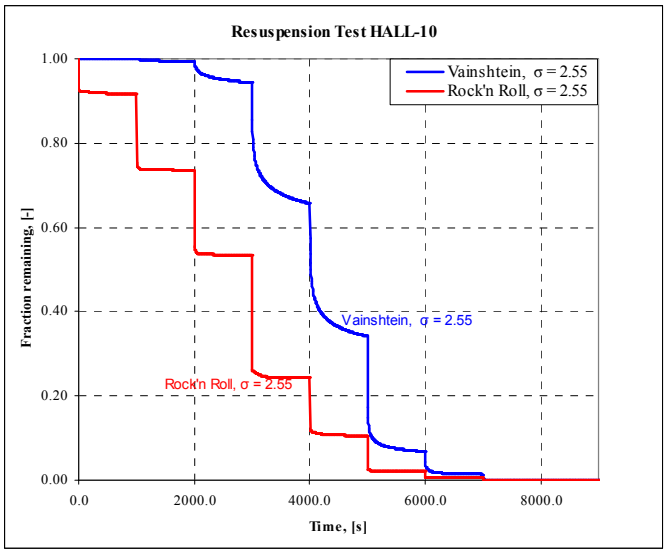

Figure 19 Reeks & Hall, 10-µm, time-dependent curves.

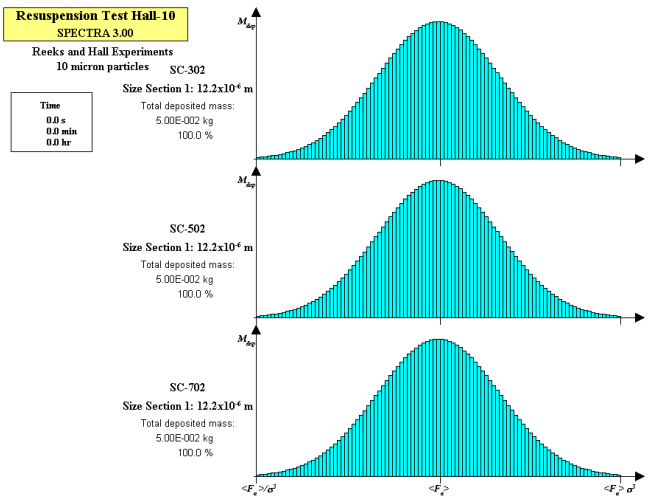

Figure 20 Reeks & Hall, 10-µm, F_a-distributions, 0.0 s.

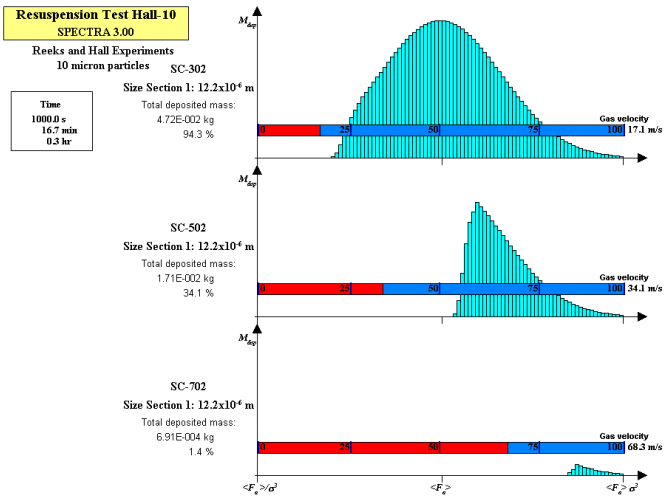

Figure 21 Reeks&Hall, 10-µm, F_a-distributions, 1000 s.

After a short resuspension period the lines become practically flat, which means that the resuspension stops until the next velocity increase step is made. In other words, the F_a-sections that are being resuspended are gone very quickly (which means that R_m is very large for these sections), while the others stay (which means that $R_m \sim 0.0$). If an "error" of a factor of 2 in the R_m calculations is made, it won't affect the sections for which $R_m \sim 0.0$. Similarly for the sections for which R_m is large there will be no visible effect; the particles from these sections will simply be swept away fraction of a second sooner or later.

An effect may be observed only in the section, which is at the "edge" of a resuspension ($0.0 < R_m < 1.0$). Thus at the worst an error of a single F_a-section resuspension is made. In the SPECTRA modeling the number of F_a-sections is typically between 51 and 99 [1]. Thus an error made by resuspending or not a single section is on the average 1÷2%, which is very small compared to the accuracy of the model against the experimental data.

Figure 20 and Figure 21 show a section-by-section distribution of the deposited particles at the start of the calculations ($t = 0.0$ s) and after 1000 s for the case:

- Vainshtein resuspension model
- Adhesion force $<F_a>$ calculation using "all defaults"
- Adhesive spread of $\sigma_a = 2.55$

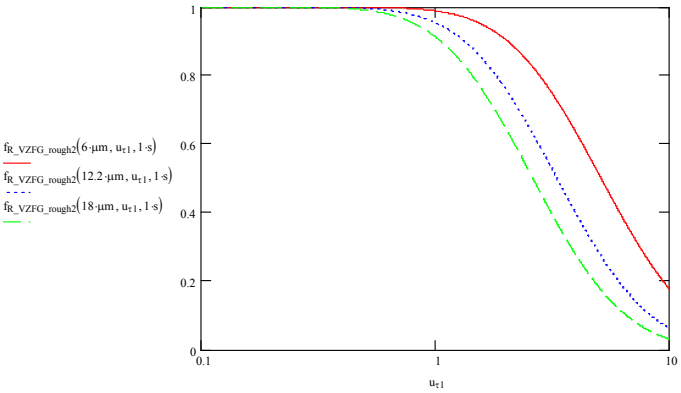

Figure 22 Reeks & Hall, 10-µm, MathCAD, $\sigma = 10.4$ [9].

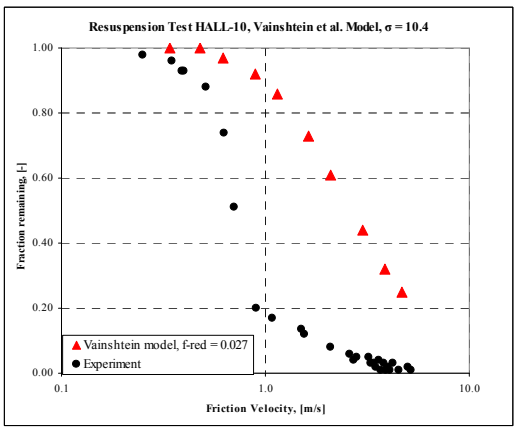

Figure 23 Reeks & Hall, 10-µm, SPECTRA.

Initially the particle distribution follows the assumed lognormal distribution (Figure 20). Figure 21 shows how the weakly bound particles (particles left hand side in these figures) are gradually swept away with the increasing gas velocity.

The results of the Vainshtein model with σ_a = 10.4 are compared to the analytical solutions obtained by means of MathCAD [9] in Figure 22 and Figure 23. The middle line in Figure 22 represents the 12.2 µm particles. SPECTRA results give slightly lower values than MathCAD. The MathCAD curves were presented for 1.0 s after an instantaneous velocity step. In SPECTRA the (stable) values obtained 1000 s after a resuspension step, are shown. It was checked in SPECTRA outputs that the remaining fraction after 1000 s are about 10% lower than at 1 s, which explains the difference between MathCAD and SPECTRA for this case.

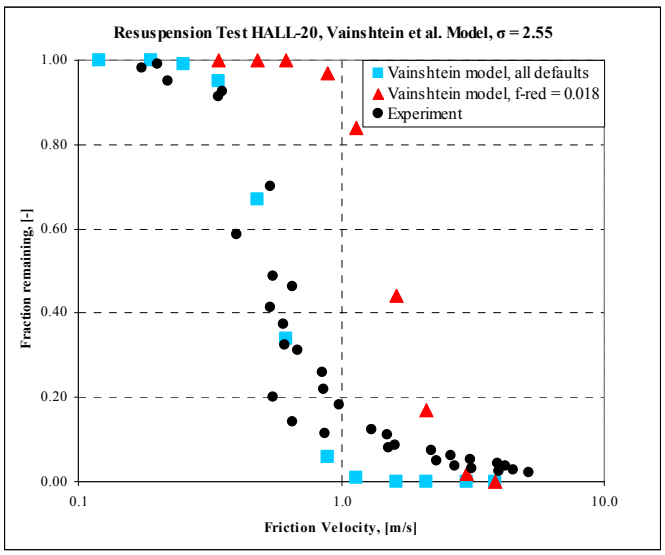

Figure 24 Reeks & Hall, 20 µm, Vainshtein, σ = 2.55.

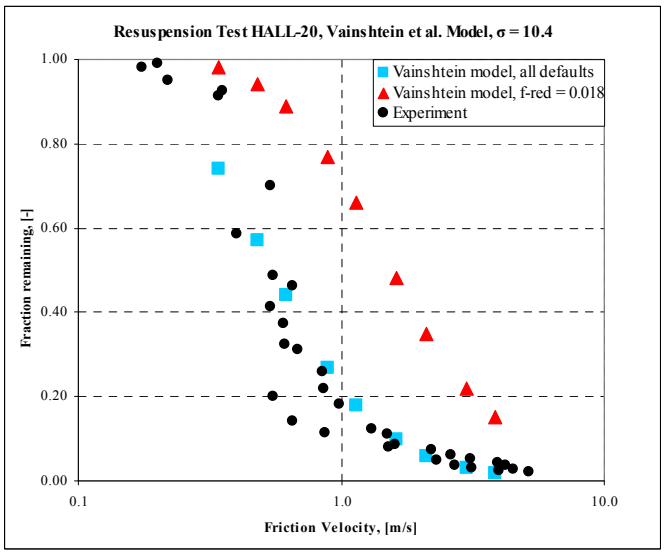

Figure 25 Reeks & Hall, 20 µm, Vainshtein, σ = 10.4.

3.2.2 "20-µm" Particles

The nominal "20-µm" particles had the mean diameter of 23 µm [7]. The same cases were analyzed as for the "10-µm" particles. Reduction factor of 0.018 is recommended for this case in [7], therefore $\langle r_{as} \rangle = 0.018 \times 23 \times 10^{-6}/2 = 2.1 \times 10^{-7}$ m.

Results are shown in Figure 24 through Figure 27. The following observations can be made:

- Results close to experimental measurement are obtained with the Vainshtein mode with default adhesion force $\langle F_a \rangle$ calculation. Results obtained with the F_a calculation through asperity size calculation with the reduction factor of f_{red} = 0.018 give too large fraction of remaining particles.
- Results obtained with the adhesive spread of σ_a = 2.55 give somewhat closer match to the experimental data than the results of σ_a = 10.4; the first gives somewhat too steep lines, the second gives not steep enough.

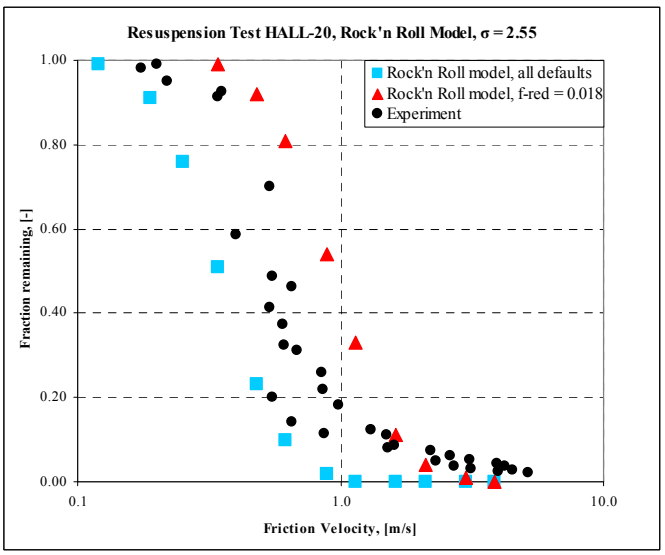

Figure 26 Reeks & Hall, 20 µm, Rock'n Roll, σ = 2.55.

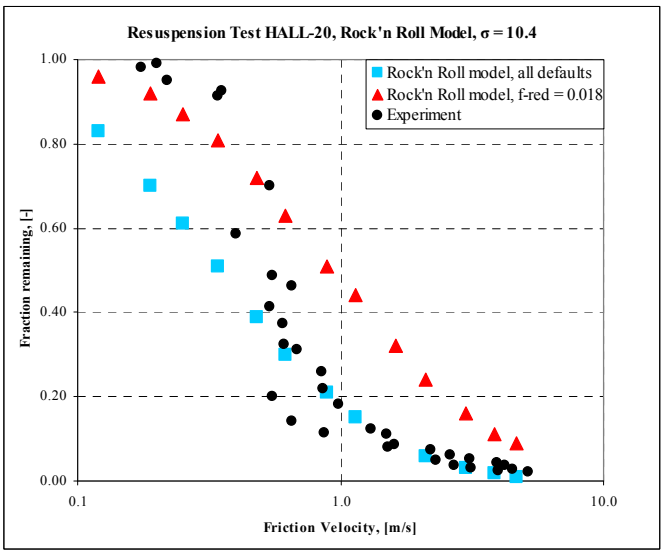

Figure 27 Reeks & Hall, 20 µm, Rock'n Roll, σ = 10.4.

- A value of adhesive spread in between the two used values is expected to give best results. Default value in SPECTRA is 4.0. Results for this value are shown in section 3.2.3.
- The Rock'n Roll model with the mean adhesion force $<F_a>$ calculated from the default correlations and σ_a = 2.55 predicted remaining fractions that are somewhat lower than in experiments. The Vainshtein model with the same assumptions gives results that are quite close to the experiment. With these assumptions results of both models are close to the measured data.

The results of the Rock'n Roll model, as calculated by SPECTRA are compared to the Rock'n Roll model, as presented in the original article of Reeks and Hall in Figure 28 and Figure 29. The case with σ_a = 10.4 and the Vainshtein et al. approach with the reduction factor of f_{red} = 0.018 is presented in the article (Figure 28), This case is shown in Figure 29 for comparison (the same case is shown in Figure 27).

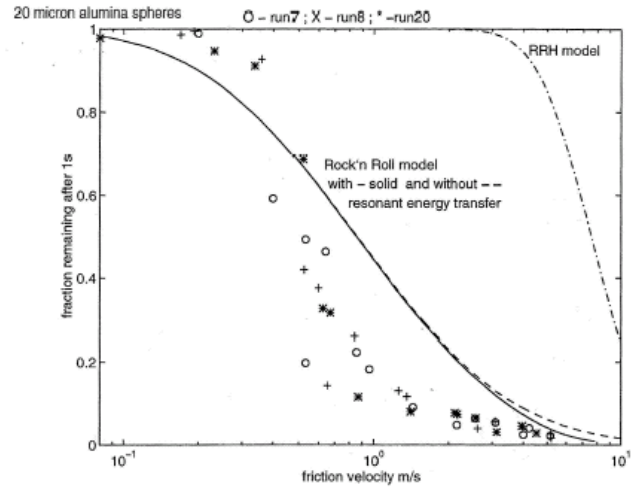

Figure 28 Reeks & Hall, 20-µm, [7].

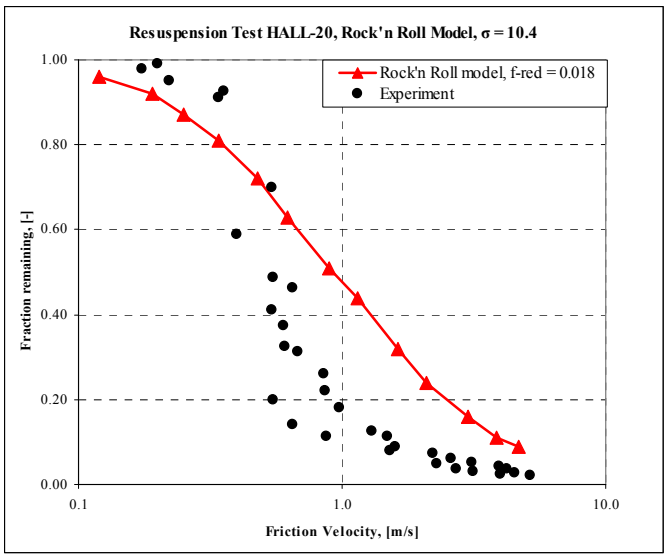

Figure 29 Reeks & Hall, 20-µm, Rock'n Roll, σ = 10.4.

SPECTRA results for this case agree well with the Rock'n Roll model data presented in [7]. The slope of the calculated results is too small compared to the experiment. This is a consequence of applying a large value of σ_a.

3.2.3 "All defaults" Resuspension Model

Results shown above for both "10-µm" and "20-µm" particles indicated that the considered adhesive spread factors of 2.55 and 10.4 bounded the expected value. The default value of the adhesive spread in SPECTRA is 4.0. It is therefore interesting to compare the results calculated with this value. For the comparison selected below, the "all default" model parameters were selected. Two resuspension models were used, the Vainshtein and the Rock'n Roll model.

Results are shown in Figure 30 and Figure 31. Both models are in good agreement with the experiment. Rock'n Roll model overestimates the resuspension in the low friction velocity region.

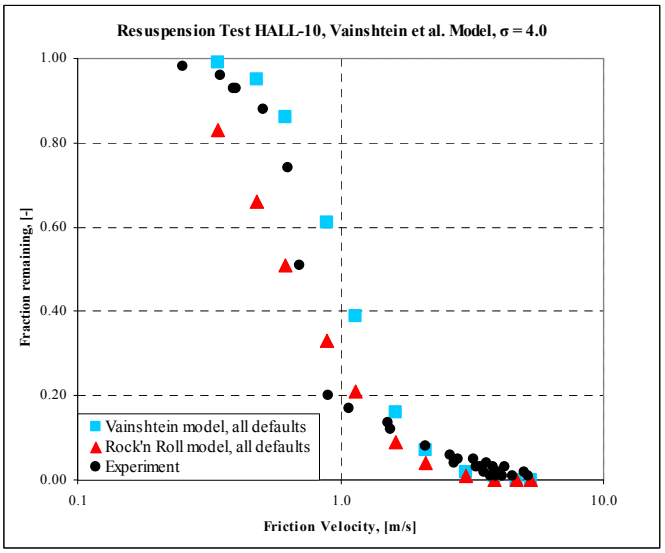

Figure 30 Reeks & Hall, 10-µm, "all defaults".

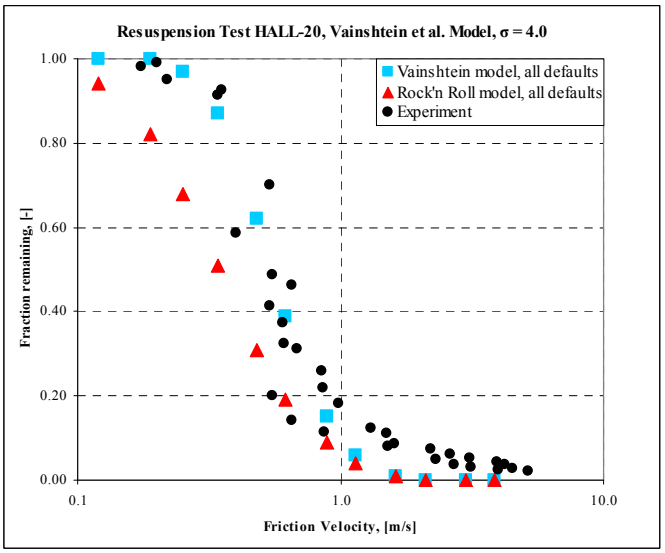

Figure 31 Reeks & Hall, 20-µm, "all defaults".

For the currently selected default parameters the Vainshtein model with "all defaults" model coefficients may be considered as a "best estimate" resuspension model, while the Rock'n Roll model with "all defaults" model coefficients may be considered as a "conservative" resuspension model. More experiments are needed in order to confirm this observation.

3.2.4 Vainshtein Model with $\langle r_{as} \rangle = 10^{-8}$ m

Results shown above for both "10-µm" and "20-µm" particles the indicated that the Vainshtein model with certain the reduction factors did not give very good results. Firstly, the obtained numbers were quite far from the measured ones. Secondly, the obtained values were not conservative, i.e. the resuspended fractions were too small compared to the experimental data. This fact is important if the models are to be applied for safety analyses of PBMR NPP.

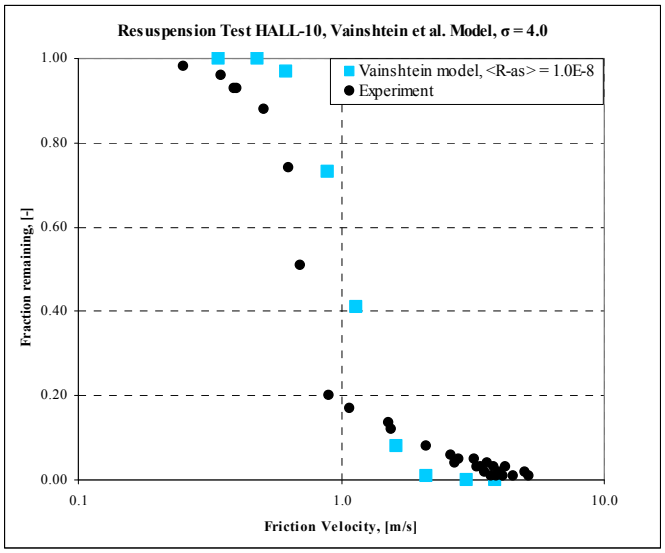

Figure 32 Reeks & Hall, 10-µm, Vainshtein, $\langle r_{as} \rangle = 10^{-8}$.

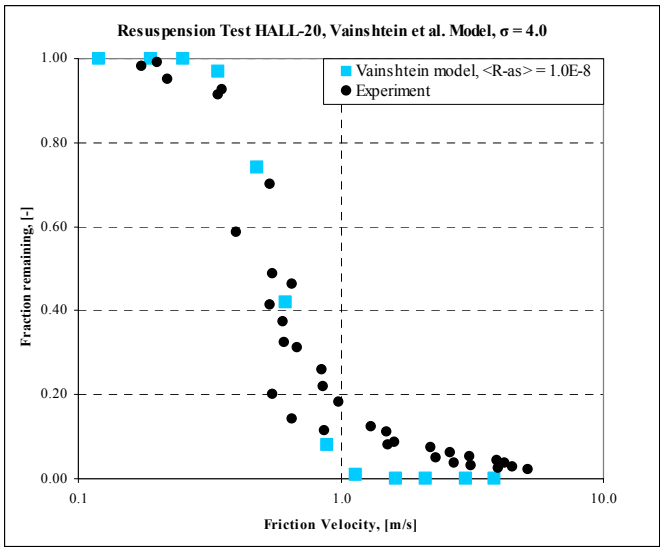

Figure 33 Reeks & Hall, 20-µm, Vainshtein, $\langle r_{as} \rangle = 10^{-8}$.

A short sensitivity study has been performed with the model in order to investigate what values of the mean asperity radius would provide a more reasonable fit to the experiment. A single value of the mean asperity radius was chosen for both "10-µm" and "20-µm" particles. Use of a single asperity radius is preferred over the use of different asperity radii for different particle sizes (as recommended in the original article of Vainshtein) because the asperity radius is a surface-related property; therefore one should not use different values for different particles. This issue is further discussed in [1].

It was found out that the mean asperity radius of $\langle r_{as} \rangle = 10^{-8}$ m gives quite a good match to the experimental data. Results are shown in Figure 32 and Figure 33.

3.3 STORM SR11 Test

The STORM experiment SR11 (ISP-40) [8] and the SPECTRA results for this test are described in reference [1]. Five particle size sections were used in the calculations, with diameters of D_p = 0.25, 0.5, 1.0, 2.0, and 4.0 µm. A lognormal particle distribution was assumed, with a mean particle diameter of $\langle D_p \rangle$ = 0.43 µm, and a standard deviation σ_p = 1.7, based on [8]. Two resuspension models were used:

- Vainshtein model.
- Rock'n Roll model (built using the "extended mechanistic model" - see section 2.9).

Three options were used:

- Adhesion force distribution (section 2.3) with mean adhesion force, $\langle F_a \rangle$, calculated using the built-in correlations (section 2.5), assuming the $R = 1.0\times10^{-5}$ m. The mean asperity radius (needed in such case only for conversion of the adhesion force, F_a, to the tangential pull-off force, F_{at}) is equal to:

$$\langle r_{as} \rangle = 1.0\times10^{-7} \text{ m}$$

- Adhesion forces calculated from the asperity distribution (section 2.4). The reduction factors were obtained from the original article [2] 0.1. This means:

$$\langle r_{as} \rangle = 0.1\times(D_p/2)$$

  The mean asperity radii used for each particle size sections are:
  - Size 1 (D_p=0.25×10^{-6} m): $\langle r_{as} \rangle$=0.125×10^{-7} m
  - Size 2 (D_p=0.50×10^{-6} m): $\langle r_{as} \rangle$=0.250×10^{-7} m
  - Size 3 (D_p=1.00×10^{-6} m): $\langle r_{as} \rangle$=0.500×10^{-7} m
  - Size 4 (D_p=2.00×10^{-6} m): $\langle r_{as} \rangle$=1.000×10^{-7} m
  - Size 5 (D_p=4.00×10^{-6} m): $\langle r_{as} \rangle$=2.000×10^{-7} m

- The same option as above, with the mean asperity radius equal to 10^{-8} m for all particle sizes. This value provided a good match to experimental data for the Reeks and Hall experiments (see section 3.2, Figure 32 and Figure 33).
- Two values od the adhesive spread factors were considered:
  - σ_a = 4.0
  - σ_a = 2.5.

Results are shown in Figure 34 through Figure 37. The following observation can be made.

- When the mean adhesion force $<F_a>$ is calculated using the built-in correlations, the resuspension is somewhat overestimated in the early resuspension steps (Figure 34, circles). When the adhesive spread of $\sigma_a = 2.5$ is used the resuspension is overestimated during all steps (Figure 34, triangles). These results indicate that the adhesion force distribution is shifted to the right (higher adhesion forces), compared to the distributions assumed here.
- The results obtained with the asperity size distribution and the Vainshtein value: $f_{red} = 0.1$ give clearly too low resuspension (Figure 35). This is consistent with the observation already made at the Reeks and Hall experiments (see section 3.2, Figure 12, Figure 13, Figure 24, and Figure 25).

Note that in case of the Reeks and Hall experiments the applied reduction factors were even lower than here (0.027 ÷ 0.018).

- Relatively good results were obtained when the adhesion forces are calculated from the asperity size, with the mean asperity radius of $<r_{as}> = 1.0\times10^{-8}$ m, applied for all particle size sections (Figure 35). It is interesting to observe that the same conclusion was reached from the Reeks and Hall experiments. This fact would indicate that when the method of Vainshtein is used, the mean asperity radius of order of 10^{-8} m is a better number than 10^{-7} m, which is being used with the default correlations. More experiments and measurement data are needed to confirm if those observations can be considered as generally applicable.

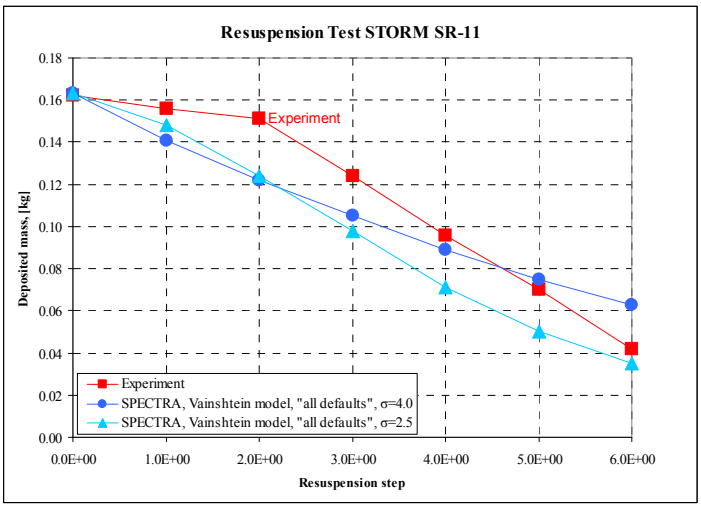

Figure 34 STORM, default F_a calculation.

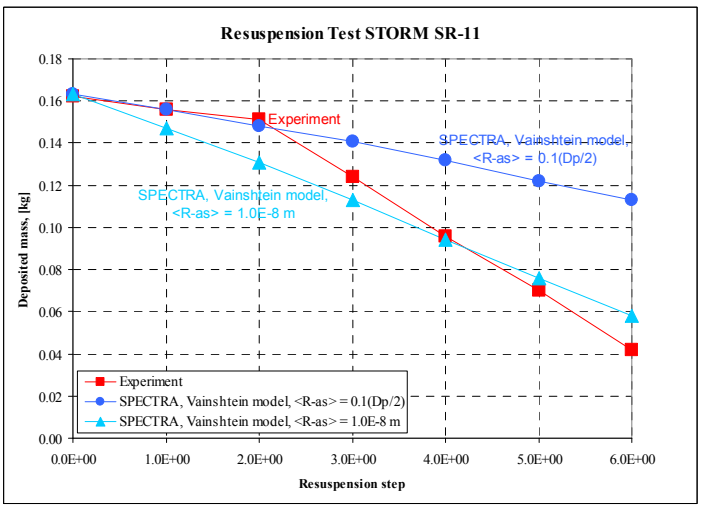

Figure 35 STORM, F_a calculation through asperities.

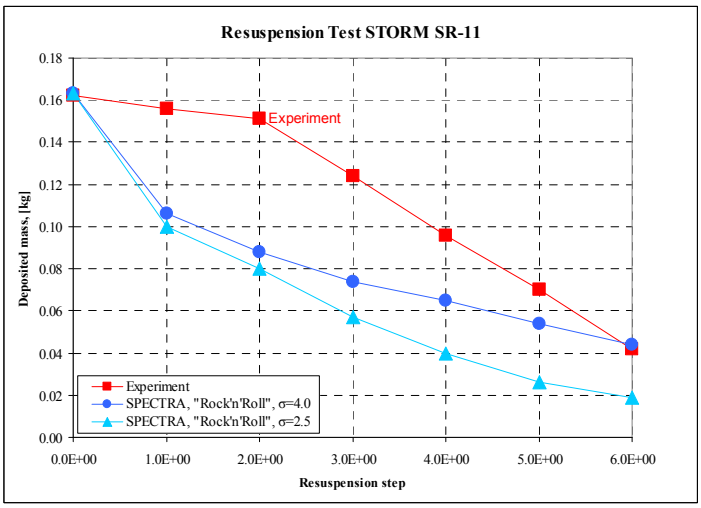

Figure 36 STORM, Rock'n Roll model.

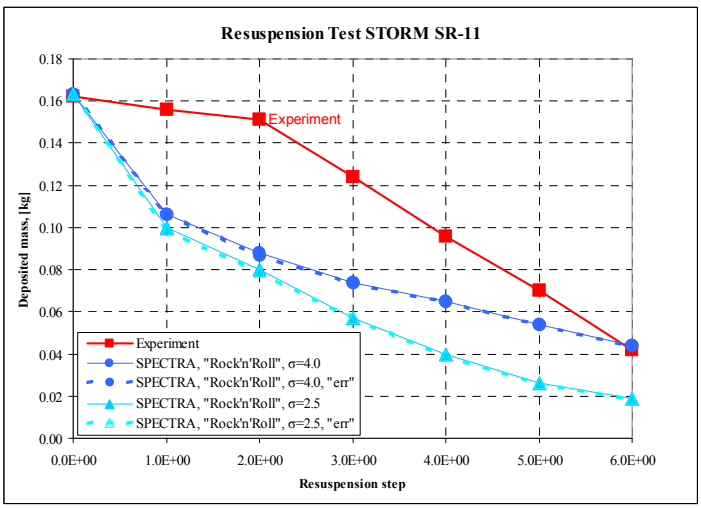

Figure 37 STORM, Rock'n Roll, influence of errf.

- The Rock'n Roll model gives too high resuspension rates (Figure 36). This is consistent with the observation already made at the Reeks and Hall experiments, where it was concluded that the Rock'n Roll model with $<F_a>$ calculated from the default correlations gives conservative results (see section 3.2, Figure 30 and Figure 31).
- The term with error function has been neglected in the Rock'n Roll model. Influence of this term on the results is investigated in the same way as in case of Reeks and Hall experiments. Bounding calculations are performed with the limiting values of the error function: $errf(0)=0$ and $errf(\infty)=1$. Results are shown in Figure 37. As in case of the Reeks and Hall experiments very small difference is found between the two bounding values of the error function.

Comparison of the adhesion force, $F_{a,}$, distributions and the tangential pull-off force, $F_{a\tau}$, distributions are shown in Figure 38 and Figure 39. The following cases are compared:

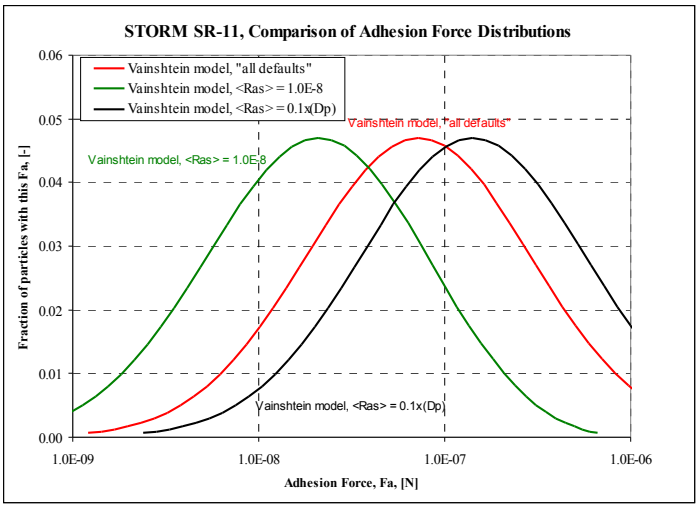

Figure 38 STORM SR11, F_a distributions.

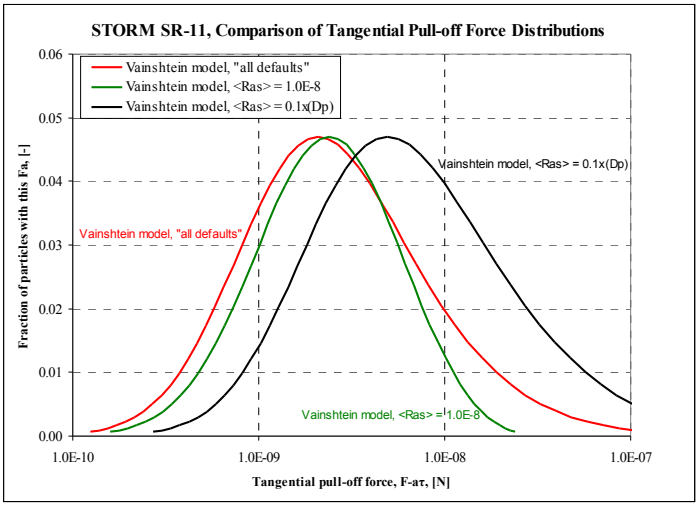

Figure 39 STORM SR11, $F_{a\tau}$ distributions.

- Default models for $<F_a>$, $<r_{as}>=10^{-7}$ m
- F_a from asperity distribution, $<r_{as}>=10^{-8}$ m
- F_a from asperity distribution, $<r_{as}>=0.1\times(D_p/2)$

Only the cases with the Vainshtein model are shown. In case of the Rock'n Roll model the default adhesion force models were used, therefore the adhesion force distribution is exactly the same as the first line shown in Figure 38. The tangential pull-off force is not used by the Rock'n Roll model, so there are no values to be shown in Figure 39.

It is seen in Figure 38 that the largest adhesion forces are observed in the case of the Vainshtein reduction factor of 0.1: $<r_{as}> = 0.1\times(D_p/2)$. The smallest forces are observed in the case with $<r_{as}> = 1.0\times10^{-8}$ m. The default models for $<F_a>$ give the values roughly in the middle between the previous two.

The Vainshtein resuspension model does not use the adhesion force, F_a, directly, but the tangential pull-off force, $F_{a\tau}$, which is calculated from the F_a. The tangential pull-off force, $F_{a\tau}$, distributions are shown in Figure 39 for the same cases for which F_a-distributions were shown. The largest pull-off forces are observed for the case with $<r_{as}> = 0.1\times(D_p/2)$. The large values of $F_{a\tau}$ result in too small resuspension in this case (Figure 35) The default $<F_a>$ correlations with $<r_{as}> = 10^{-7}$ m give very similar results as the use of the asperity size distribution with $<r_{as}> = 10^{-8}$ m. Both these cases give good agreement with experiment (Figure 34 and Figure 35).

It may seem surprising that the case with $<r_{as}> = 10^{-8}$ m exhibits similar values of $F_{a\tau}$ as the default case, while it gives the smallest adhesion force, F_a. It is explained as follows. $F_{a\tau}$ is proportional to $(F_a)^{3/2}$ and inversely proportional to $(D_{eff,0})^{2/3}$ (see reference [1]):

$$F_{a\tau} \sim \frac{F_a^{3/2}}{r_{as}^{2/3}}$$

When the asperity radius is made smaller, then with the same value of F_a, a larger value of $F_{a\tau}$ is obtained. Therefore the $F_{a\tau}$ is in the third case similar to the one obtained in the second case, while the F_a is much smaller in the third case compared to the second case.

4 SUMMARY

NRG has performed a review of available resuspension models. The dynamic resuspension models of Vainshtein et al., Reeks Reed and Hall (RRH), and the Rock'n Roll model were reviewed in more detail. A dynamic resuspension model based on Vainshtein et al. was selected for implementation into a thermal-hydraulic system code. The resuspension model formulation of Vainshtein et al. has been extended in such way that other formulations (for example the Rock'n Roll model) may easily be defined and used within the general model framework.

The developed resuspension model has been implemented into the SPECTRA thermal-hydraulic system code. Verification and validation of the new code version has been performed. The code verification includes comparisons of the numerical SPECTRA results with the analytical solutions obtained by means of MathCAD.

The performed verification runs show:

- The agreement between the MathCAD results and SPECTRA results is very good, even for very short times when a careful calculation procedure is applied to match closely the instantaneous velocity step in MathCAD. This agreement proves that the equations were correctly coded in SPECTRA; therefore the model is verified.

The validation includes comparisons with the experimental results of the Reeks and Hall and STORM experiments. Analysis of the Reeks and Hall experiments has shown that:

- Vainshtein model with the built-in correlations for the adhesion force and adhesive spread of 4.0 gives very good agreement with the experiments.
- Rock'n Roll model with the built-in correlations for the adhesion force and an adhesive spread of 4.0 gives somewhat too fast resuspension.
- Vainshtein model with the adhesion force calculated through the asperity size and an adhesive spread of 4.0 gives good agreement with the experiments for the mean asperity size of:

$$\langle r_{as} \rangle = 10^{-8} \text{ m}$$

- Vainshtein model with the reduction factor of 0.018÷0.027 (recommended in [7]), which means:

$$\langle r_{as} \rangle = 1.6 \times 10^{-7} - 2.1 \times 10^{-7} \text{ m}$$

leads to too low resuspension.

Analysis of the STORM experiment SR11 has shown that:

- Vainshtein model with the built-in correlations for the adhesion force and adhesive spread of 4.0 gives very good agreement with the STORM experiment.
- Rock'n Roll model with the built-in correlations for the adhesion force and adhesive spread of 4.0 gives somewhat too fast resuspension.
- Vainshtein model with the adhesion force calculated through the asperity size and an adhesive spread of 4.0 gives good agreement with the STORM experiment for the mean asperity size of:

$$\langle r_{as} \rangle = 10^{-8} \text{ m}$$

- Vainshtein model with the reduction factor of 0.1 (recommended in [2]), which means:

$$\langle r_{as} \rangle = 0.125 \times 10^{-7} - 2.0 \times 10^{-7} \text{ m}$$

leads to too low resuspension.

The observations are very similar for both Reeks and Hall, and STORM experiments. More experiments and measurement data are needed to confirm if those observations can be considered as generally applicable.

5 CONCLUSIONS

Both the Vainshtein the Rock'n Roll model, applied with "all defaults" model coefficients, give good results of the analyzed Reeks and Hall and STORM experiments. The Rock'n Roll model gives somewhat more conservative results (higher resuspension).

The Vainshtein model with the mean reduction factor of 0.1, which means $\langle r_{as} \rangle = 0.1 \times D_p$, leads to too optimistic results (too low resuspension). Since the obtained values are not conservative the model should not be applied for safety analyses of a Nuclear Power Plant. Better results are obtained with the mean asperity size of $\langle r_{as} \rangle = 10^{-8}$ m, independently of the particle size. More experiments and measurement data are needed to confirm this observation.

A key factor in successful resuspension predictions is a good knowledge of the adhesion force and its distribution for dust particles deposited on rough surfaces. Theoretical considerations may lead to helpful expressions for the adhesive forces under a variety of conditions. However they cannot be reliably used yet for the assessment of the safety of a Nuclear Power Plant. Therefore, experimental data is needed that will allow to obtain adhesion force distribution for the materials and corresponding surfaces roughness of the components in an actual PBMR plant. Such experiments will make it possible to calibrate the model, by supplying the adhesion force data, and to verify the developed model. Such experiments will be performed by PBMR. The experiments may lead to an adjustment of some user-defined parameters in the current model, in order to obtain a generally applicable best estimate and conservative resuspension models.

NOMENCLATURE

Symbols

D_{eff} effective particle diameter, [m]
D_p particle diameter, [m]
D_p^+ dimensionless particle diameter, [-]
E_p Young modulus, particle [Pa]
E_s Young modulus, surface [Pa]
f friction factor, [-]
f_0 frequency of vibration, [s^{-1}]
f_{red} reduction factor, [-], (used when the adhesion force distribution is determined from the asperity size distribution in the Vainshtein resuspension model)
F_a adhesive force, [N]
$\langle F_a \rangle$ mean value of the adhesive force, [N]
$F_{a\tau}$ tangential pull-off force, [N]
F_d drag force, as used by the model, [N]
F_d' drag force, source formula, [N]
F_L lift force, as used by the model, [N]
F_L' lift force, source formula, [N]
H relative humidity, [-]
m deposited mass, [kg]
r_{as} asperity radius, [m]
$\langle r_{as} \rangle$ mean value of the asperity radius, [m]
R surface roughness [m]
R_m resuspension rate computed by the present model, fraction of deposited particles resuspended per second, $R_m = (1/m)(dm/dt)$, [s^{-1}]
R_p particle radius, [m]
u_τ friction velocity, [m/s]
V_g gas velocity, [m/s]

Greek symbols

μ_g viscosity of gas, [kg/m/s]
ν_p Poisson's ratio, particle, [-]
ν_s Poisson's ratio, surface, [-]
ρ_g density of gas, [kg/m^3]
σ_a adhesive spread factor (standard deviation of the log-normal distribution), [-]
σ_{as} asperity spread factor (standard deviation of the log-normal distribution), [-]
φ distribution function, [N^{-1}]

REFERENCES

[1] M.M. Stempniewicz, "SPECTRA Sophisticated Plant Evaluation Code for Thermal-Hydraulic Response Assessment, Version 3.00, December 2005, Volume 1 – Program Description, Volume 2 – User's Guide, Volume 3 – Subroutine Description, Volume 4 - Verification and Validation", NRG report K5020/04.61079, Arnhem December 2005.

[2] P. Vainshtein, G. Ziskind, M. Fichman, C. Gutfinger, "Kinetic Model of Particle Resuspension by Drag Force", *Physical Review Letters*, Vol. **78**, No. 3, pp. 551 - 554, 1997.

[3] M.W. Reeks, J. Reed, D. Hall, "On the Resuspension of Small Particles by a Turbulent Flow", *Journal of Physics D: Applied Physics*, Vol. 21, pp. 574-589, 1988.

[4] E.M.J. Komen, "Dispersion of Fission Products and Dust in Direct Cycle HTRs", NRG report 21346/06.01.31/C, Petten 2006.

[5] E.Hontanon, A. de los Reyes, J.A. Capitao, "The CÆSAR Code for Aerosol Resuspension in Turbulent Pipe Flows. Assessment Against the STORM Experiments", *J. Aerosol Sci.* Vol. **31**, No. 9, pp. 1061-1076, 2000.

[6] E.M.J. Komen, "PBMR Resuspension Analyses, Main Coolant Lines", NRG report, Draft, March 2006.

[7] M.W. Reeks, D. Hall, "Kinetic models for particle resuspension in turbulent flows: theory and measurement", *Aerosol Science*, **32**, 1-31, 2001.

[8] A.R. Costelo, J.A. Capitao, G.D. Santi, "International Standard Problem 40 – Aerosol Deposition and Resuspension, Final Comparison Report", OECD NEA/CSNI/R(99)4, February 1999.

[9] E.M.J. Komen, "Resuspension Analysis, Hall Experiment", NRG report, Draft, March 2006.